Vehicle dynamic modeling and stability program active front steering sliding mode integrated control

Ashkan Behmanesh

***Abstract*—This document describes the simulation and results of the research conducted by Xiaobin Fan et al [1], titled Vehicle dynamic modeling and stability program active front steering sliding mode integrated control. The models and controllers in the reference paper are used to establish an ESP and AFS controller for the vehicle. Based on the equations on the paper, the vehicle model and controllers are designed. although the information about simulation conditions is not enough, we could find similar patterns for results through simulation.**

I. Introduction

ACTIVE front steering (AFS) and electronic stability program (ESP) are active safety devices for vehicles to improve vehicle handling and stability. In the linear range of the tire lateral force, the vehicle can intervene more directly and quickly through the AFS, and the energy required and tire wear is so small as to be difficult for a driver to detect. This differs from the nonlinear range of automobile tires, where the control effect of ESP is obvious. Xiaobin Fan et al focused on the implementation of the algorithm and real vehicle verification. they tried to reach to satisfy the robustness of the control algorithm. So, in their study, a precise vehicle high-dimensional nonlinear dynamic model and a tire dynamic friction model were established. AFS, ESP, and coordinated control algorithms were designed. However, this paper focuses on controller parts which contain a simulation of AFS and ESP.

II. Vehicle Dynamics Modeling

In this section, the vehicle nonlinear multi-degree of freedom dynamics model is developed, which includes the body, steering system, braking system, and tire subsystem model. we will discuss each one of these subjects briefly.

A. Vehicle body dynamics model

The body dynamics model was established as Fig. 1, which includes longitudinal motion, lateral motion, yaw motion, and roll motion. longitudinal, lateral, and vertical forces, yaw moment, lateral and longitudinal load transfer, etc computed by vehicle body dynamic equations. One of the most important parameters which are used to design AFS and ESP controllers is Yaw angle ψ and lateral acceleration A_y.

B. Wheel dynamics model

The dynamic equations of the driving wheel are as follows.

$$\dot{\omega}_i = \frac{1}{I_{Wi}}[T_i - RF_{ti} - T_{brki} - d_i F_{zi}] \tag{1}$$

where R is the wheel rolling radius. I_{Wi} is the wheel equivalent moment of inertia. T_i is the input drive torque. T_{brki} is braking torque. d_i is the offset of wheel normal force and F_{ti} is the tire longitudinal force.

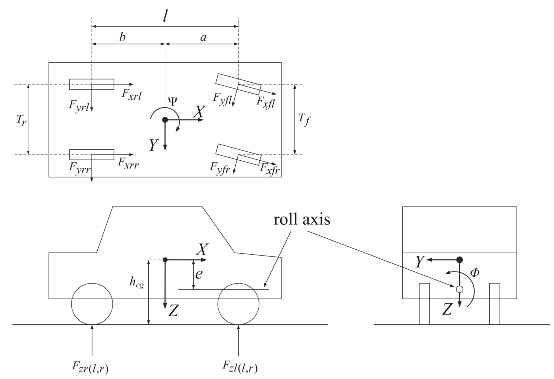

Fig. 1: Vehicle body dynamics model.

C. Tire dynamic friction model

The tire's mechanical properties have an important influence on vehicle handling stability, braking safety, and ride comfort. The development of modern automobile dynamics needs to establish an accurate tire model that reflects the tire's physical essence. Four different models are used to simulate tire behavior as real as possible. The models are:

1) Dugoff tire model
2) Magic formula tire model
3) Tire brush model
4) Tire LuGre dynamic friction model

To compare the results of the mentioned model, a reference model(205/55R16) is used and other models are used to simulate the reference model. The simulations were conducted in different situations. Figure 2 shows the longitudinal force comparison of each tire model. In the end, the LuGre dynamic friction tire model was found preferable because it reflects the tire response characteristics not even in linear sections, but also the transient behavior is well simulated using this model.

1) Tire LuGre dynamic friction model: The tire LuGre dynamic model can not only describe the Stribeck effect and the pre-slip effect of the tire friction process but also can describe the effect of the change separation force and the friction hysteresis effect [3]. The two frictional contact surfaces are assumed to be two rigid bodies that contact each other through some so-called elastic bristles. When one of these contacts exerts a tangential force along the contact surface, the bristles will deflect as springs, and cause friction on the contact surface to increase. If the frictional force is sufficiently large, the “mane” over deflection will occur and slip occurs. LuGre dynamic friction model is shown in

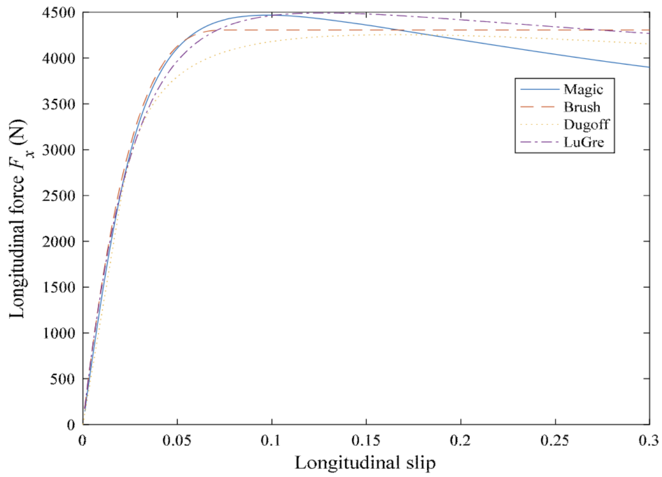

Fig. 2: Longitudinal force comparison of each tire model.

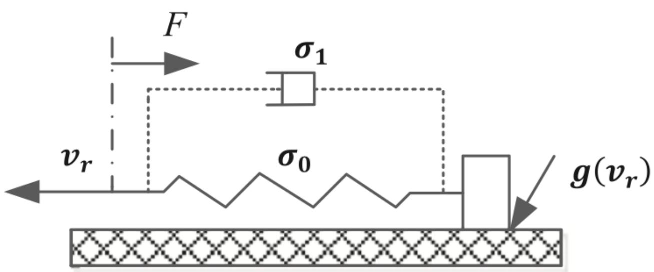

Fig. 3: LuGre dynamic friction model.

figure 3. This model defines the frictional force as below:

$$F = \sigma_0 z + \sigma_1 \frac{dz}{dt} + \sigma_2 v_r \tag{2}$$

Where σ_0 is the tire longitudinal stiffness coefficient, σ_1 is the tire longitudinal damping coefficient, σ_2 is the viscous damping coefficient and z is the average elastic deflection of mane. Also, z is a function of relative velocity of contact surface (v_r), sliding friction function $g(v_r)$, and total drive ratio of Powertrain (ζ). The final deformation equation of bristle deformation z can be obtained as follows.

$$\frac{\partial z}{\partial t} = v_r - \frac{\partial \sigma_0 |v_r|}{\partial g(v_r)} z - r|\omega| \frac{\partial z}{\partial \zeta} \tag{3}$$

In this research, we use steady-state situation to model the vehicle. By putting $\frac{\partial z}{\partial t} = 0$ in equation 3, the steady state analytical solution can be obtained.

III. AFS/ESP INTEGRATED CONTROL SYSTEM

In order to calculate the vehicle ideal state, a linear two degrees of freedom model is established, which includes lateral motion and yaw motion, and is shown in figure 4. The paper has used the single track model dynamic equations to find $\dot{\beta}$ and $\dot{r}$. The equations are following.

$$\begin{bmatrix} \dot{\beta} \\ \dot{r} \end{bmatrix} = \begin{bmatrix} a_{11} & a_{12} \\ a_{21} & a_{22} \end{bmatrix} \begin{bmatrix} \beta \\ r \end{bmatrix} + \begin{bmatrix} b_1 \\ b_2 \end{bmatrix} \delta \tag{4}$$

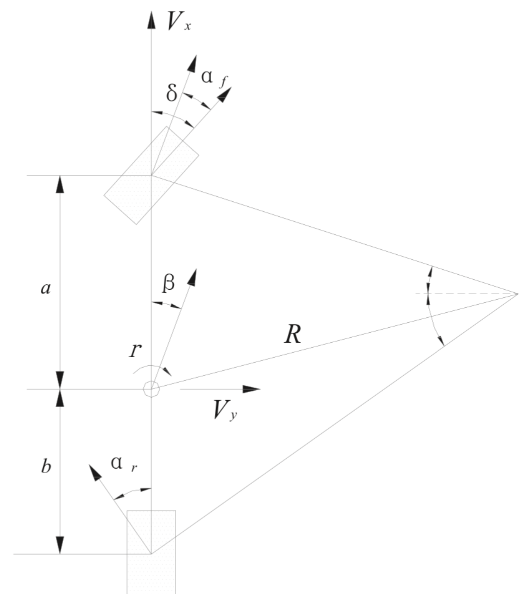

Fig. 4: Linear two degrees of freedom model.

Where δ is steering angle, β is side slip angle and r is yaw rate. Also, the parameters of equation 4 are:

$$a_{11} = \frac{-2 \cdot C_{af} - 2 \cdot C_{ar}}{m \cdot u}$$
$$a_{12} = -1 + \frac{2 \cdot C_{ar} \cdot b - 2 \cdot C_{af} \cdot a}{m \cdot u^2}$$
$$a_{21} = \frac{2 \cdot C_{ar} \cdot b - 2 \cdot C_{af} \cdot a}{I_{zz}}$$
$$a_{22} = \frac{-2 \cdot C_{af} \cdot a^2 - 2 \cdot C_{ar} \cdot b^2}{I_{zz} \cdot u}$$
$$b_1 = \frac{2 \cdot Caf}{m \cdot u}, b_2 = \frac{2 \cdot Caf \cdot a}{I_{zz}}$$

Where C_{ar} and C_{af} is the cornering stiffness of the rear and front tire, m is vehicle mass, u is vehicle longitudinal velocity, a is the distance between the center of mass and front axle, b is the distance between the center of mass and rear axle, and I_{zz} is yaw moment of inertia.

From this model, we can compute the steady-state model by putting $\dot{\beta} = 0$ and $\dot{r} = 0$. When doing circular motion, the yaw speed of the vehicle is limited by the condition of the road surface adhesion, so there is the maximum allowable yaw angular velocity. We used the lateral acceleration to calculate the maximum yaw rate where $a_y = v_x r + \dot{v_y}$. $\dot{v_y}$ can be written as $v_y = v_x \tan(\beta)$. Then a_y can be expressed as $a_y = v_x r + \dot{v_x} \tan(\beta) + \frac{v_x \dot{\beta}}{\sqrt{1+\tan^2 \beta}}$. The lateral acceleration at the tire attachment limit must be met $|a_y| \leq \mu g$.

The maximum yaw rate can be expressed by the approximate formula $r_{uplim} = 0.85 |\frac{\mu g}{V_x}|$. In this way, the ideal yaw rate r_d is equal to:

$$r_d = \min[|r_{ss}|, |r_{uplim}|].\text{sign}(\delta) \tag{5}$$

The same approach can be used to find β_d. The empirical formula of limit side slip angle is $\beta_{up_lim} = tan^{-1}(0.02\mu.g)$. , so the ideal side slip angle is as follows.

$$\beta_d = \min[|\beta_{ss}|, |\beta_{uplim}|] \tag{6}$$

A. AFS control logic

This paper tries to implement the AFS system by tracking the error between the actual and desired yaw rate. The tracking error is $e_c = r - r_d$ and its rate is $\dot{e_c} = \dot{r} - \dot{r_d}$. Also, The sliding surface can be defined as $s = e_c$. The sliding mode dynamics of the system are as follows.

$$\dot{s} = -\lambda s \tag{7}$$

where, λ is positive constant. Now we can use this equation into vehicle model equations (equation 4) and find the control rule for steering angle which is the following.

$$\delta = \left(\frac{1}{b_2}\right)(-a_{21}\beta - a_{22}r + \dot{r}_d - \lambda s) - \text{sign}(s) \cdot \chi \tag{8}$$

where, χ is the control gain, which determines the speed of the system when it reaches the slip surface. In this paper, we assumed $\chi = 1$.Then the additional input angle of AFS is $\Delta\delta = \rho_c.(\delta - \delta_d)$, ρ_c is the coordination control parameter, δ_d is front wheel desired angle by the driver.

B. Coordinated control algorithm

The switching control algorithm is adopted in this paper. For a convenient handle in engineering, setting $\beta_d = 0$. We design The value of ρ_c as a function of β and $\dot{\beta}$. So a function is defined that switches the controller works based on the output of this condition. The function is the following.

$$\text{Cond} = |\kappa_1\dot{\beta} - \kappa_2\beta| \tag{9}$$

κ_1 and κ_2 can be tuned to modify the effect of $\dot{\beta}$ and β on the switching control algorithm. In this paper, we tried to determine the range of β and $\dot{\beta}$ and based on the value of these ranges, select κ_1 and κ_2. After testing different values of parameters, we decided to put $\kappa_1 = 50$ and $\kappa_2 = 100$.
There is the following formula that determines the switching controller behavior based on equation 9 and other tunable parameters. The value of ρ_c is shown in the following formula.

$$\rho_c = \begin{cases} 0 & \text{for} \quad Cond < B1 \\ \frac{B2-Cond}{B2-B1} & \text{for} \quad B1 \leq Cond \leq B2 \\ 1 & \text{for} \quad Cond > B2 \end{cases} \tag{10}$$

B1 and B2 represent the definition of a stable region and can be obtained by experimentation. After testing different values of parameters, we put B1 = 23 and B2 = 5. In figure 6, we can see the actual activation function for vehicle with Step steer input at u = 100 km/h. Of course, the activation function figure is different for every scenario.
Figure 5, shows the logic of activating ESP or AFS controller. Based on this logic, if the value of ρ_c is equal to 1, the vehicle is controlled by AFS only and all wheels rotate with no disturbance from ESP. However, if $\rho_c = 0$ or $1-\rho_c = 1$, AFS

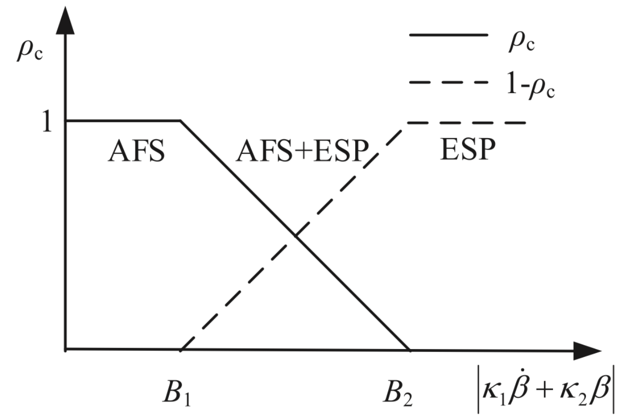

Fig. 5: Coordination control characteristics.

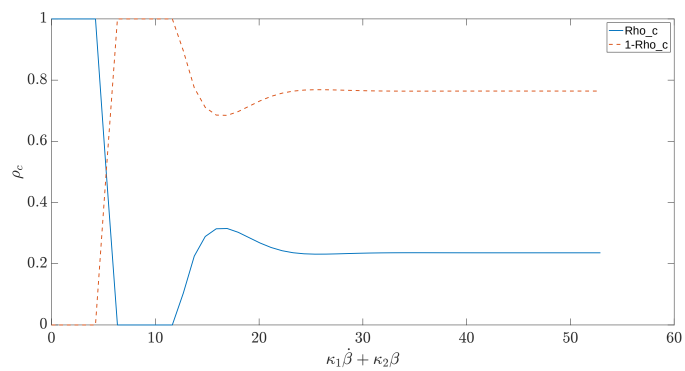

Fig. 6: Coordination control characteristics for step steer input at $u = 100km/h$

does not interrupt vehicle steering and lets the ESP control the vehicle by applying the appropriate yaw moment to the vehicle. If ρ_c is between 0 and 1, both ESP and AFS try to control the vehicle. According to the condition function value, the system assigns the proper control level and distributes the control level between AFS and ESP.

C. ESP

the ESP system applies selective braking to individual wheels to counteract oversteer or understeer situations, helping the driver maintain control and prevent skidding or sliding. By actively intervening in critical moments, ESP enhances overall vehicle stability and reduces the risk of accidents, particularly during sudden maneuvers or slippery surfaces. The simple selection principle of the active braking wheel is shown in Table. In this paper, a simple control rule is used, that is, this control method can provide the compensation torque well so as to control the vehicle stability.

To simulate the table I, we used a State machine in Matlab Simulink. The steering angle (δ_d) and the difference between the rear and front axle (in single track model, the difference between the rear and front tire) side slip angle ($\Delta\alpha = \alpha_r - \alpha_f$) are used as the input. As soon as $\Delta\alpha$ takes a value other than

δ	e_c	Direction of Steering Wheel	Steering Characteristics	Brake Wheel Selection
+	+	Right	Oversteer	Left front wheel
+	−	Right	Understeer	Right rear wheel
−	+	Left	Oversteer	Right front wheel
−	−	Left	Understeer	Left rear wheel

TABLE I: Coordination control characteristics.

0, the ESP tries to lead $\Delta\alpha$ to 0 again so the vehicle can naturally steer again.
The ESP approach in this paper, is based on the required yaw moment (M_z) to keep the vehicle in natural steering behavior. the M_z can be calculated based on the derivative of lateral and longitudinal forces over time ($\frac{dF_{xi}}{dt}$ and $\frac{dF_y}{dt}$). According to Table I, in the event that the vehicle is oversteered, it is necessary to brake on the outer front wheel, and the yaw moment Δ_{Mz} is obtained as follows.

$$\begin{aligned}\Delta_{Mz} = \Delta_{Fx}\left(\frac{1}{2}\cdot Tw\cdot\cos(\delta) + a\cdot\sin(\delta)\right)\\ - \Delta_{Fy}\left(a\cdot\cos(\delta) - \frac{1}{2}\cdot Tw\cdot\sin(\delta)\right)\end{aligned} \tag{11}$$

During understeering situations, braking is applied to the inner rear wheel, and the yaw moment Δ_{Mz} is obtained as follows.

$$\Delta_{Mz} = (\Delta_{Fx}\cdot 0.5\cdot Tw) - (\Delta_{Fy}\cdot b) \tag{12}$$

Based on equation 11 and 12, we can find the required yaw moment to avoid the vehicle losing control. By applying Δ_{Mz} to the vehicle, we can keep the vehicle in a stable situation.

IV. Simulation comparison

A. Paper results

According to the above AFS, ESP, and integrated control logic, simulation analysis is carried out. In the main Paper, the simulations were conducted as follows.

- Sine wave steering input
  1) Scenario 1) High adhesion coefficient road (μ=0.9, initial speed u0=100 km/h)
  2) Scenario 2) Low adhesion coefficient road (μ=0.2, initial speed u0=60 km/h)
- Step function steering input
  1) Scenario 3) High adhesion coefficient road (μ=0.9, initial speed u0=100 km/h)
  2) Scenario 4) Low adhesion coefficient road (μ, initial speed u0=60 km/h)

Based on the figures in the paper for the mentioned tests, in the first scenario, AFS and ESP systems can reduce vehicle yaw rate 7 and control side slip angle 8. In both papers, the same pattern is observed. Both AFS and ESP are capable of controlling vehicle yaw rate separately, but when both systems are active together, the best results are obtained. In scenario 2, vehicle is moving in low friction condition. in this case, when vehicle tries to do a sinusoid maneuver,

but as seen in figure 10, vehicle can not be controlled without AFS/ESP and β angle doesn't follow the maneuver anymore, while when both ESP and AFS are activated, the vehicle follows the maneuver trajectory. please note that the yaw rate of vehicle without a controller looks lower than the yaw rate with ESP/AFS activated 9. In this case, this yaw rate is not correct because the vehicle is slipping. Same pattern can be observed in reference paper [1]. However in that case, due to vehicle characteristics, not controlled vehicle side slip angle doesn't drift away from desired one. But in both cases, ESP and AFS controllers can maintain the vehicle in the desired situation.

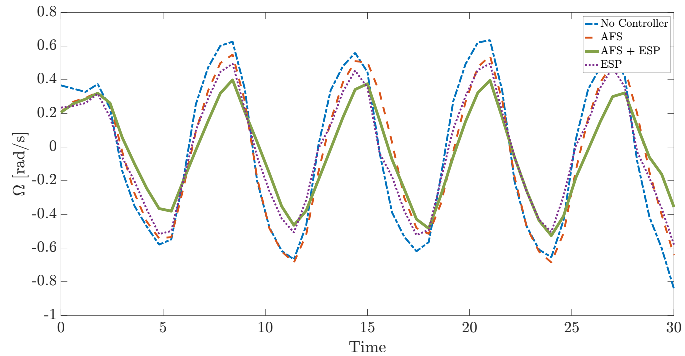

(a)

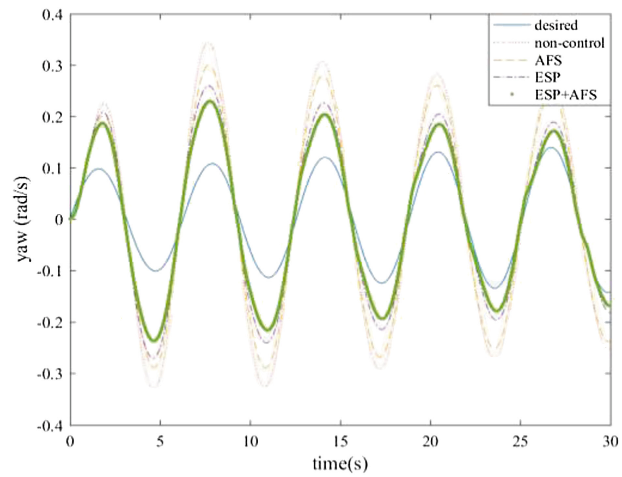

(b)

Fig. 7: Scenario 1- yaw rate of Simulation(a) and reference (b)

In single-step steering function, simulation results show the same pattern as the reference paper in both High and Low friction situations. Based on figure 11 and, 12, in high friction condition, vehicle can handle the situation and follow the maneuver. However, using ESP/AFS can help the vehicle to optimize vehicle behavior and show more precise reaction to the input steering. On the other hand, the effects of ESP/AFS is more visible in low friction condition. according to 13, vehicle behavior can be optimized not only in yaw rate but also in the required time to get stable.

Based on discussed results, tests results can approve the reference results [1]. However, due to different vehicle pa-

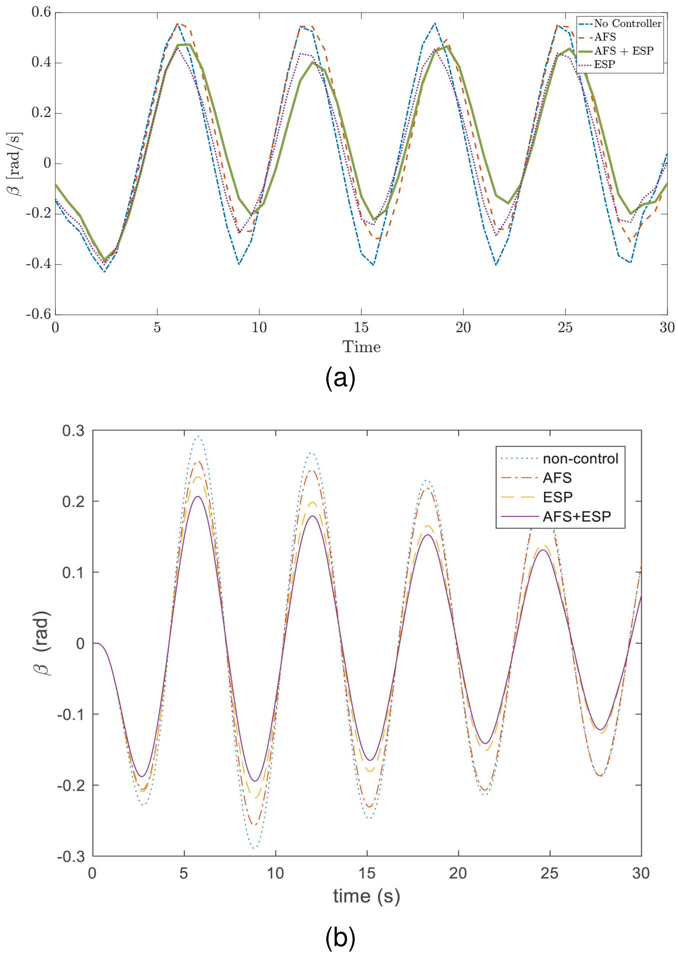

Fig. 8: Scenario 1- Slip angle of Simulation(a) and reference (b)

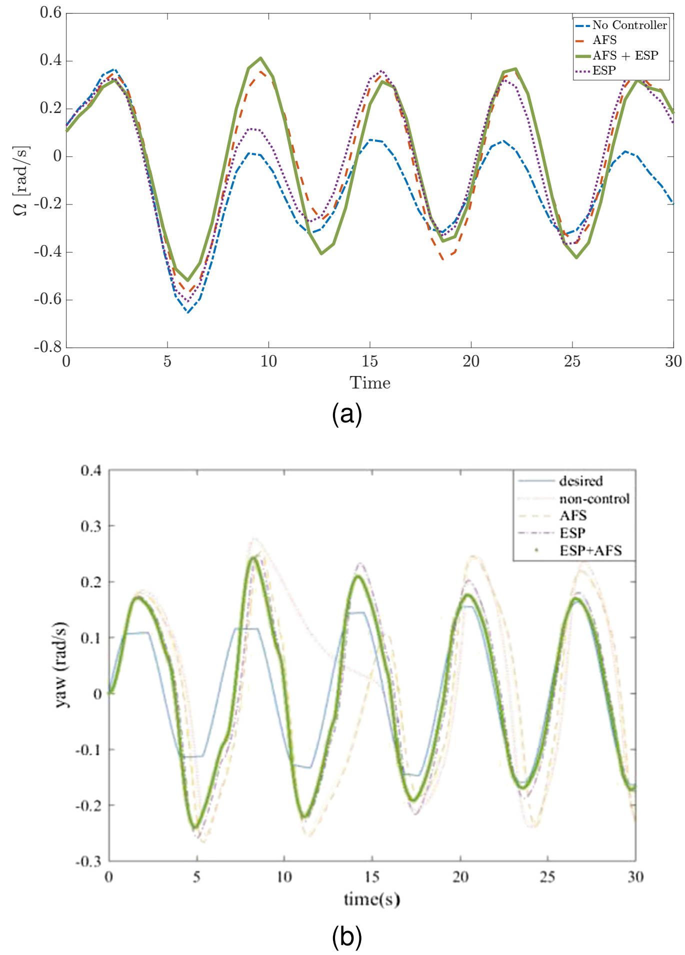

Fig. 9: Scenario 2- yaw rate of Simulation(a) and reference (b)

rameters, small differences can be observed in the results, but the pattern shows that the ESP/AFS systems are working in an effective way.

V. Conclusion

The multi-degree of freedom nonlinear dynamic vehicle model was built first. A comparative study was conducted with the magic formula tire model, Dugoff tire model, brush tire model, and LuGre dynamic friction tire model and the steady state tire model based on LuGre. However, the pre-defined Matlab double-track vehicle model is used for designing AFS and ESP controllers. An AFS controller was designed based on vehicle model and parameters like yaw rate, side slip angle and longitudinal and lateral velocity. The outcome of AFS is steering modification so the vehicle can keep yaw rate and side slip angle close to desired ones.ESP controller does the same task by controlling yaw moment of the vehicle. ESP calculate the required yaw moment based on derivative of wheels' longitudinal and lateral force and velocity, steering direction and steering behavior of the vehicle. Requested yaw moment can be applied to the vehicle by controlling wheels velocity or braking torque of each wheel. Moreover, an coordinated control algorithm is developed to control the performance of AFS and ESP. During some conditions, especially low friction roads, the controllers can not control the vehicle very well. coordinated control algorithm finds the best control distribution between AFS and ESP and if one of them performs poorly, the algorithm keeps it out of the system and lets the other one controls the vehicle. In most of the conditions, however, the coordinated control algorithm tries to use both controllers but limits the effect of each one based on vehicle condition. In the end, simulations were conducted to test controller's performance in different scenarios. We defined some scenarios to test the controllers under different road conditions and steering inputs, such as sinusoidal or step steering. According to the results of the tests, controllers can keep the vehicle in stable condition and avoid unpredictable motions while in some scenarios, vehicle would lose control if the AFS/ESP is disabled. It is also possible to use ESP and AFS in circumstances where the vehicle does not require controllers to follow the maneuver in order to optimize the vehicle's motion and find the best solution to follow the required trajectory without using controllers. As is obvious, ESP and AFS can reduce the range of yaw rate and side slip angle so the vehicle can move more stable.

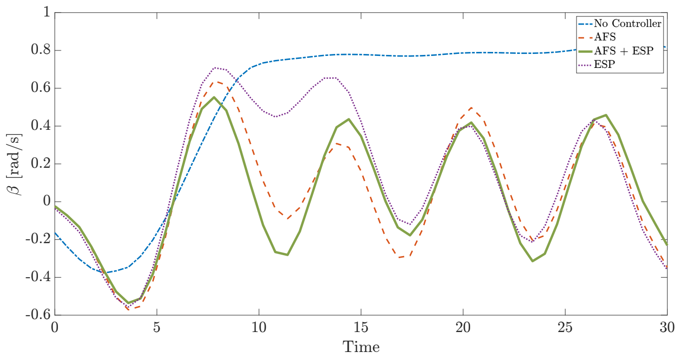

(a)

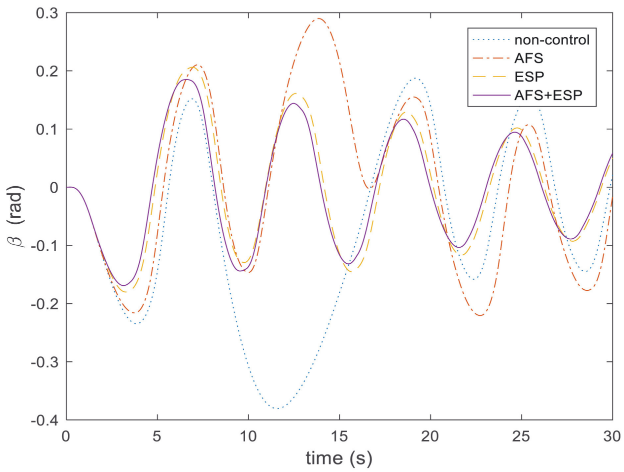

(b)

Fig. 10: Scenario 2- Slip angle of Simulation(a) and reference (b)

REFERENCES

[1] Xiaobin Fan and Zixiang Zhao*VEHICLE DYNAMICS MODELING AND ELECTRONIC STABILITY PROGRAM/ ACTIVE FRONT STEERING SLIDING MODE INTEGRATED CONTROL*. 2018 Chinese Automatic Control Society and John Wiley and Sons Australia, Ltd.

[2] *The MathWorks, Inc.* (2022). Optimization Toolbox version: 9.4 (R2022b). 2018 Chinese Automatic Control Society and John Wiley Sons Australia, Ltd.

[3] Tsiotras, P., E. Velenis, and M. Sorine*A LuGre tire friction model with exact aggregate dynamics* (2004). Vehicle System Dynamics, Vol. 42, No. 3, pp. 195–210

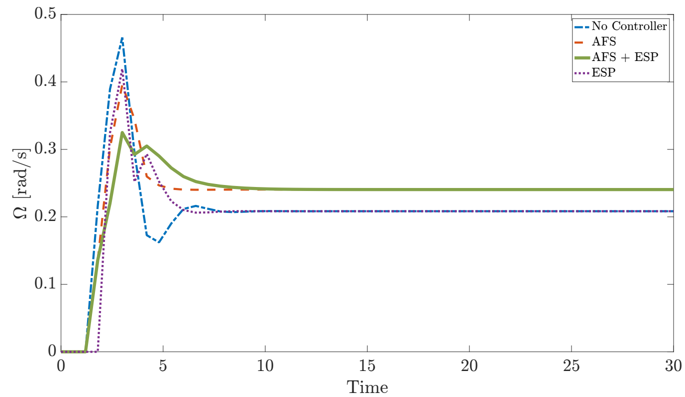

(a)

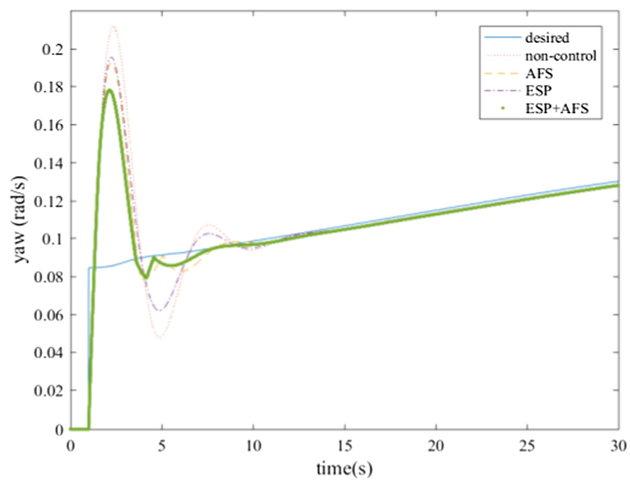

(b)

Fig. 11: Scenario 3- yaw rate of Simulation(a) and reference (b)

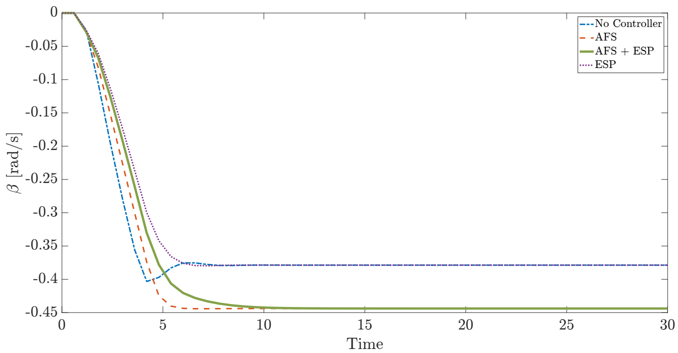

(a)

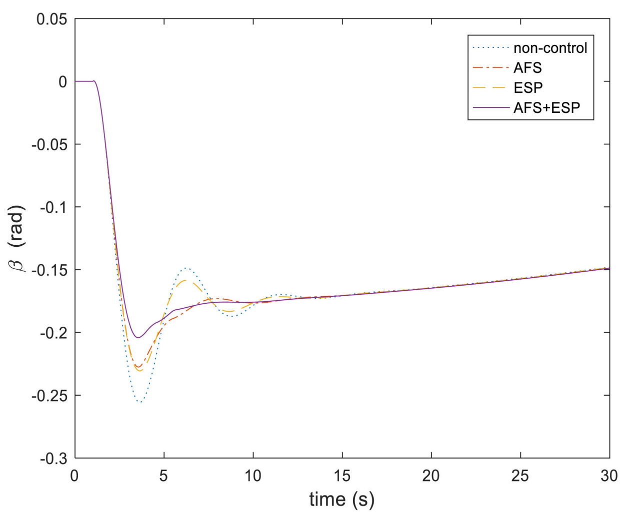

(b)

Fig. 12: Scenario 3- Slip angle of Simulation(a) and reference (b)

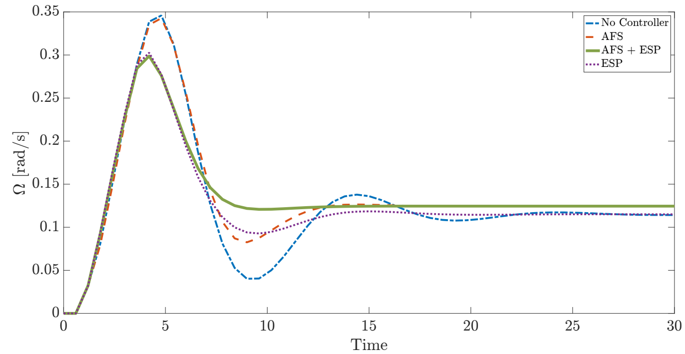

(a)

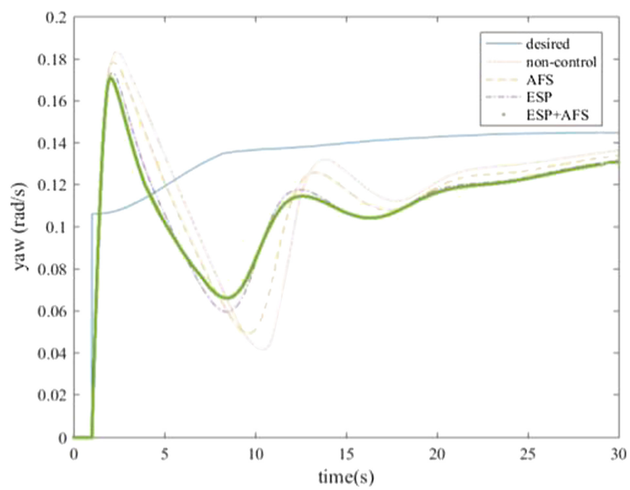

(b)

Fig. 13: Scenario 4- yaw rate of Simulation(a) and reference (b)

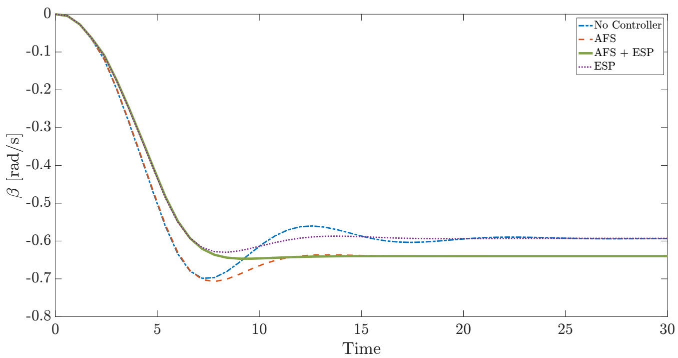

(a)

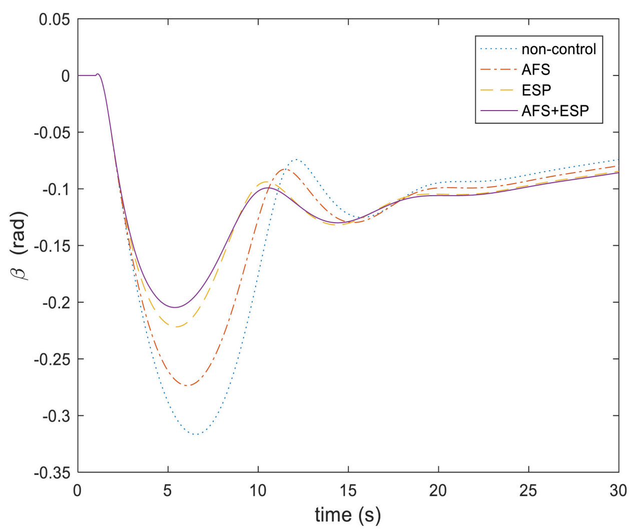

(b)

Fig. 14: Scenario 4- Slip angle of Simulation(a) and reference (b)